High Temperature Oxidation of Cr-Steel Interconnects in Solid Oxide Fuel Cells

Saeed Ghali, Azza Ahmed, Taha Mattar

Abstract—Solid Oxide Fuel Cell (SOFC) is a promising solution for the energy resources leakage. Ferritic stainless steel becomes a suitable candidate for the SOFCs interconnects due to the recent advancements. Different steel alloys were designed to satisfy the needed characteristics in SOFCs interconnect as conductivity, thermal expansion and corrosion resistance. Refractory elements were used as alloying elements to satisfy the needed properties. The oxidation behaviour of the developed alloys was studied where the samples were heated for long time period at the maximum operating temperature to simulate the real working conditions. The formed scale and oxidized surface were investigated by SEM. Microstructure examination was carried out for some selected steel grades. The effect of alloying elements on the behaviour of the proposed interconnects material and the performance during the working conditions of the cells are explored and discussed. Refractory metals alloying of chromium steel seems to satisfy the needed characteristics in metallic interconnects.

Keywords—SOFCs, Cr-steel, interconnects, oxidation.

I. INTRODUCTION

SOFCs are currently being developed to replace the conventional combustion technology [1], [2] because of their low emission, high efficiencies, fuel flexibility, and potential electricity/heat cogeneration, etc. However, there is still needed work to improve the economics and reduce the cost of the manufacturing of this new developed SOFCs.

Traditional SOFCs work at high temperatures, around 1000 °C. At this temperature, the interconnect material is conventionally made of a ceramic material, such as $La1-xCaxCrO_3$ [3]. However, these ceramic interconnects are difficult to manufacture, which limits the application in SOFCs. Ceramic interconnects also have low electrical conductivity and are expensive.

Recent research has enabled to decrease the operating temperature of the SOFC from 1000 to 800-600 °C. This progress has been made by reducing the thickness of the electrolyte [4] and modifying the Triple Phases Boundaries (TPB) reaction of cathode electrolyte interface into Internal Diffusion mechanism (ID) reaction [5]. The lower operating temperature authorises metallic alloys as possible candidates for interconnects [3]. Metallic materials have higher electrical and thermal conductivities, are easier to fabricate, and, in general, have lower cost compared to the ceramic interconnects [3], [6]. Chromium is the most important element because of the formation of chromia as protective and semiconducting layer. The presence of other elements could improve the characteristics of this layer, limiting the growth rate and the acceptable area-specific resistance (ASR), reducing the poisoning of the electrodes due to the oxidation gaseous species (CrO_3 or $CrO_2(OH)_2$) at temperatures close to 1000 °C and higher [7]-[9], but also observed at lower temperatures due to the severe operation conditions, such as the presence of water vapour [7], [8], [10], [11]. The formation of a protective, single-phase chromia layer requires high chromium content of about 17-20% [6], [12]-[14]. The determination of exact chromium content depends on the percentage of other alloying elements and different processing conditions. Mn and Ti are used in low quantities (less than 0.5%) to improve the oxidation resistance. Mn tends to form a Cr–Mn spinel on the external surface layer to decrease the formation of volatile Cr species [6], [7], [13], [15]-[17]. Elements such as molybdenum and tungsten can also be added to match better thermal expansion coefficient of the alloys to those of other fuel cell components. The amount of aluminum and silicon must be kept low to prevent the formation of their insulating oxides, alumina and silica. Oxidation of different grades of stainless steel at high temperature – ranging from 500 °C up to 800 °C was investigated [18]. Also, the contribution of different alloying elements, time and temperature on oxidation behavior was illustrated [19].

The challenge in using such materials is the possibility of evaporation of chromium from the oxide layer on the surface [20]. So, this work aims to investigate the oxidation behaviors of developed high chromium ferritic steel with different additives of alloying elements as Mn, Al, Ti, Nb, V, Mo at maximum working temperature.
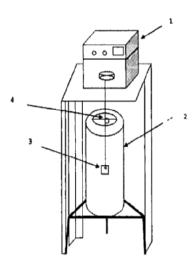
II. EXPERIMENTAL

18 ferritic stainless steels with different additives were melted in induction furnace of capacity 10 kg and cast in sand mold. Complete chemical analysis has been carried out for all cast steels. The cast steels were normalized at 1000 °C for 4 hours, followed by free forging. Ingots with square diameter 65 mm were hot forged to about 35 mm square. The steels were reheated up to 1200 °C and hold for 2 hours then forged. Start forging temperature was 1150 °C while end forging temperature was 950 °C.

Isothermal oxidation tests were carried out for the developed stainless steels at different temperatures in air using apparatus as given in Fig. 1. It is composed of a digital thermo-balance (1), which measures the mass change to 4 decimal places accuracy. The pan of the balance is connected to Kanthal wire (nickel-chrome) which ends with a hook. The

Saeed Ghali*, Azza Ahmed and Taha Mattar are with the Central Metallurgical R & D Institute (CMRDI), Cairo, Egypt (*Corresponding author; e-mail: a3708052@gmail.com).

sample was hanged, from a hole, in a wire made from nickel-chrome, and placed inside the furnace (2) at the hot zone of the furnace. The heating rate was 50 °C mind and the temperature deviation was smaller than ± 0.9 °C. The mass of the sample is recorded as a function of time. The hook connecting the sample is hanged to the hook connected to the balance (4). The sample was placed inside the furnace after the temperature of the furnace reaches the equilibrium value of the test ± 2-3 °C. The temperature was regulated using Heraeus temperature control system, Germany. This uses Pt/Pt-Rh thermocouple which is placed in the furnace at the hot zone where the sample was hanged. The furnace was switched on and left almost for 30 minutes before placing the sample to ensure that the equilibrium temperature has reached.

Specimens, prior to oxidation tests, were cut from the forged bar in the form of 2-3 mm thick rectangular shaped samples (24 x 24 mm), polished using 80 down to 1000 grit SiC paper and ultrasonically cleaned in acetone.

The mass gain was measured for samples exposed to air at temperature 800 °C for different time intervals, up to around 1000 hrs. The samples were used in duplicates to take the average, which were hanged using nickel-chromium wire at the heat affected zone of the furnace. This wire was connected to digital sensitive balance at the times of each test. Microstructure examination of different steel grades was carried out. Scanning Electron Microscope was used to scan the surface of ferritic steels after oxidation test.

1. Digital balance

2. Electric furnace

3. Steel sample

4. Hook to hang the samples

Fig. 1 Schematic representation of the system used for high temperature oxidation of investigated steels in air

III. RESULTS & DISCUSSIONS

The aim of this article is to investigate the oxidation behaviour of developed high chromium ferritic steels in oxidative medium at maximum working temperatures. The investigated ferritic steels have different chromium content and additives. So, they are classified according to chromium content into four groups as given in Tables I-IV.

The developed chromium steels have ferritic structure as shown from examined of microstructure as given in Figs. 2 (a)-(d) for four the groups respectively.

TABLE I
CHEMICAL COMPOSITION OF FERRITIC STAINLESS STEEL WITH CHROMIUM CONTENT 28.81 – 33.01 %, WT. %

	Heat No.	C	Si	Mn	Cr	Mo	Al	Nb	Ti	V
1	1	0.0599	2	0.616	33.01	0.0517	0.0001	0.004	0.00365	0.0433
14	11	0.0626	2.64	0.266	30.46	0.0515	0.655	0.0004	0.0107	0.042
12	9	0.0782	1.25	0.828	28.81	0.0427	0.0105	0.0076	0.0923	0.0283

TABLE II
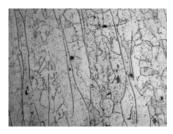CHEMICAL COMPOSITION OF FERRITIC STAINLESS STEEL WITH CHROMIUM CONTENT 25.71 – 27.31 %, WT. %

	Heat No.	C	Si	Mn	Cr	Mo	Al	Nb	Ti	V
9	6	0.0713	0.619	0.749	27.31	0.0534	1.10	0.0049	0.00489	0.0359
15	11A	0.0506	0.431	0.173	27.13	0.0544	1.57	0.0044	0.00673	0.0258
13	10	0.0859	0.55	0.714	26.35	0.0431	0.0039	0.476	0.00408	0.0272
16	11B	0.0608	0.488	0.747	26.03	0.0485	0.0584	0.0019	0.0103	0.0303
11	8	0.0641	0.388	0.132	25.90	1.04	0.0117	0.375	0.00332	0.0185
6	3A	0.0669	0.288	0.144	25.94	0.05	0.0256	0.002	0.0781	0.0237
10	7	0.0546	1.05	0.128	25.71	0.909	0.0105	0.0303	0.00829	0.0241

TABLE III
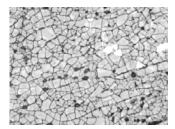CHEMICAL COMPOSITION OF FERRITIC STAINLESS STEEL WITH CHROMIUM CONTENT 25.05 – 25.16%, WT. %

	Heat No.	C	Si	Mn	Cr	Mo	Al	Nb	Ti	V
2	1A	0.0786	0.354	1.55	25.16	0.0598	0.0005	0.0029	0.00306	0.029
18	13	0.0601	0.369	0.365	25.13	1.00	0.0131	0.0053	0.0196	0.0270
17	12	0.0762	0.383	1.41	25.1	1.16	0.0217	0.0026	0.0032	0.0249
4	2A	0.0624	0.268	0.157	25.05	0.918	0.0152	0.0018	0.00303	0.0193

TABLE IV
CHEMICAL COMPOSITION OF FERRITIC STAINLESS STEEL WITH CHROMIUM CONTENT 22.11 – 23.49 %, WT. %
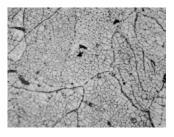
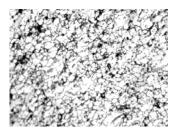|	Heat No.	C	Si	Mn	Cr	Mo	Al	Nb	Ti	V
7	4	0.226	0.337	0.0949	23.49	0.0536	0.0009	0.350	0.00251	0.0232
3	2	0.177	0.366	0.0821	23.43	1.15	0.0167	0.0051	0.00319	0.0177
8	5	0.101	2.20	0.853	23.30	0.906	0.0212	0.619	0.0602	0.0356
5	3	0.0648	1.13	0.0808	22.11	0.0491	0.0072	0.0057	0.0029	0.0514

(a) Steel (1) (first group) 10X

(b) Steel (7) (second group) 20X

(c) Steel (2A) (Third group) 20X

(d) Steel (4) (Fourth group) 20X

Fig. 2 Microstructure of developed chromium steels

Scheaffler diagram is used to estimate the phase stability of developed steels according to (1), (2) [21]. The estimated chromium and nickel equivalent of the investigated stainless steels are given in Table V. From (1), (2), the chemical compositions of different stainless steel of four steel groups, it is clear that all investigated steel grades (four groups) are belonging to stable ferritic structure region as it is illustrated in Figs. 3-6 of four groups respectively.

$$Creq = Cr + 1.5Mo + 1.5W + 0.48Si + 2.3V + 1.7Nb + 2.5A1 \quad (1)$$

$$Nieq = Ni + Co + 0.1Mn - 0.01Mn^2 + 18N + 30 C \quad (2)$$

TABLE V
CR EQUIVALENT AND NI-EQUIVALENT OF FOUR GROUPS

| No.	Cr equivalent	Ni equivalent
First group		
1	34.15419	1.85244
14	33.53923	1.90194
12	29.57831	2.42052
Second group		
9	30.52812	2.20641
15	30.22751	2.02047
13	27.56016	2.64126
16	26.55591	1.89123
11	28.35554	1.93488
6	26.07143	2.16324
10	27.71069	1.64952
Third group		
2	25.4925	2.4975
8	26.91098	1.83585
7	27.13978	2.4129
4	26.64109	1.88613
Fourth group		
7	24.38277	6.788541
3	25.42181	5.317389
8	26.90218	3.10677
5	22.80296	1.951272
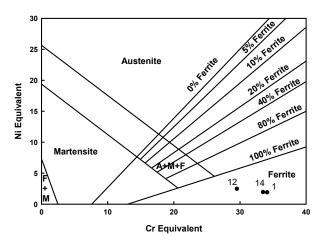
Fig. 3 Schaeffler diagram of first group, with (mass%), A= austenite, M martensite, F= ferrite of steels 1,14 & 12

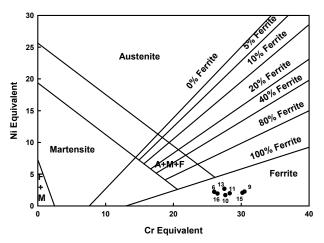Fig. 6 Schaeffler diagram of fourth group, with (mass%), A= austenite, M martensite, F= ferrite of steels 7, 3, 8 & 5

Fig. 4 Schaeffler diagram of second group, with (mass%), A= austenite, M martensite, F= ferrite of steels 9, 15, 13, 16, 11, 6 & 10
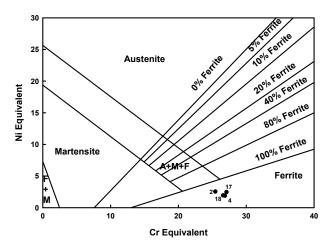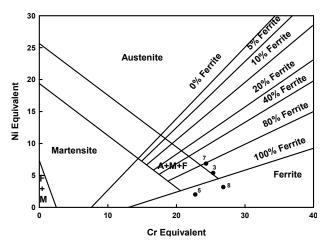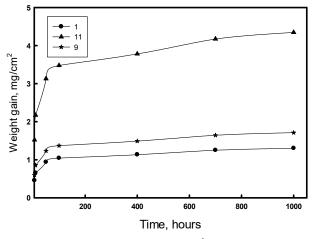

Fig. 7 The variation of mass gain (mg/cm^2) with time (hours) of steels 1, 11 and 9 at 800 $^{\circ}$C up to 1000 hour

Fig. 5 Schaeffler diagram of third group, with (mass%), A= austenite, M martensite, F= ferrite of steels 2, 18, 17 & 4
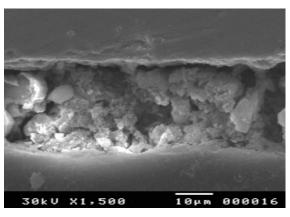

Fig. 8 SEM micrograph of steel (11)

Fig. 7 shows the variation of the mass gain (mg/cm^2) at 800 $^{\circ}$C, with time for the steels containing chromium in the range 28.8-33.01% with different additives of silicon, aluminium, manganese and vanadium. This figure shows that the mass

gain of all investigated steels, increases by time up to not more than 4.5 mg/cm^2 after 1000 hours. It is clear from Fig. 7 that the mass gain increases rapidly almost at the start up to about 50 hours, after that the rate of mass gain decreases showing almost a constant steady state. The value of the steady state mass gain is clearly dependent on the chemical composition of the investigated steels. The oxidation rate depends on the additives of alloying elements, where steel (11) which has high percent from silicon and aluminium, has higher mass gain. This observation can be demonstrated on the fact that both silicon and aluminium form silicon chromium oxides and alumina-chromium oxides [22]. It is noted that steel (9) has less mass gain. This may be attributed the presence of titanium (0.09%) – where titanium improves the oxidation resistance [23]. The mass gain (Δm), here, expresses the mass of the film remained on the surface. It has to be observed that the metal proportions lost from the base material are consumed in making the oxide film due to oxidation and some portion of this film may be lost as a spelled part. The film becomes more protective when it reaches a critical thickness at which the diffusion is minimized and where the film is less porous. The formed film is more adherent and more crystalline. SEM examination illustrated that the oxidation layer of steel (11) is about 30 μm as illustrated in Fig. 8.

Fig. 9 demonstrates the oxidation behaviour of second steel group (chromium content ranging from 25.5-27.3%). The investigated ferritic stainless steels have different alloying elements with different contents. It is obvious that the oxidation rate at the first time is fast. Mass gain (oxidation rate) after 50 hours is very small. It is clear that steel (A11) has highest oxidation rate (highest mass gain). This could be attributed to the high aluminium content (1.57%).

Steel (6) has much smaller mass gain than steel (A11), this can be attributed to that steel (6) has higher content of vanadium (0.036%) than steel (11A) (0.026%). One can conclude that V improves oxidation behavior of steel even at high Al content.

The effect of both vanadium and niobium in the presence of molybdenum can be detected by comparison between the oxidation behaviour of steels (7) & (8). It is clear that steel (7) (0.024%V) has mass gain less than steel (8) (0.018%V), even steel (8) has high niobium content (0.375%). So, it can be concluded that vanadium is more significant than niobium in improving oxidation resistance in presence of molybdenum. It is clear that mass gain of steel (10) is less than steel (8). Steels (8) & (10) have high content of Nb but steel (8) has Mo (1.04%). This is attributed to the higher content of vanadium in steel (10) (0.024%V) than in steel (8) (0.018%V). Also, it can be concluded that molybdenum has insignificant effect on oxidation behaviour.

The effect of titanium can be demonstrated through the comparison between the oxidation behaviour of steels (10) & (11B), where they have nearly the same chemical composition. It is clear that steel (11B) is more oxidation resistant than steel (10). This is due to the presence of titanium in steel (11B).

Fig. 9 shows that steel (A3) has less oxidation resistance

than steel (11B) even, the first contains more titanium. This is due to the combination effect of both manganese and silicon in steel (11B), where manganese Mn tends to form a Cr–Mn spinel on the external surface layer to decrease the formation of volatile Cr species [7], [8], [14], [16]-[18]. SEM examination illustrated that the oxidation layer of steel (7) is not more than 5 μm as illustrated in Fig. 10.
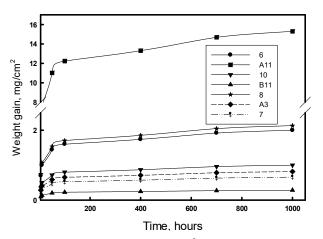

Fig. 9 The variation of mass gain (mg/cm^2) with time (hours) of steel grades of second group (6, A11, 10, B11, 8, A3 & 7) at 800 °C up to 1000 hour
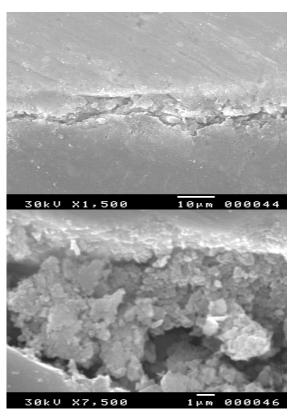
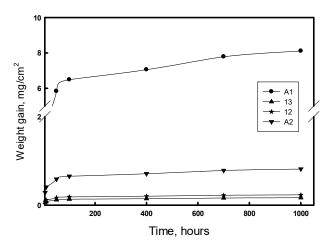

Fig. 10 SEM micrograph of steel (7)

Fig. 11 The variation of mass gain (mg/cm^2) with time (hours) of steel grades of third group (A1, 13, 12, A2) at 800 ^{o}C up to 1000 hour
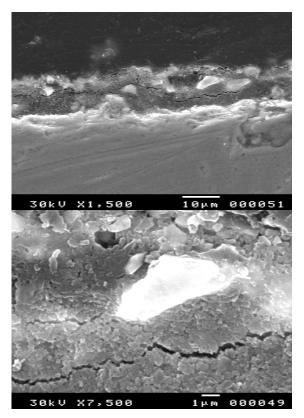

Fig. 12 SEM micrograph of steel (2)

Fig. 11 illustrates the oxidation behaviour of ferritic stainless steel with chromium content 25.0-25.13%. As mentioned before, the oxidation rate (mass gain) is faster at the first 50 hour, then reaches to steady state after about 100 hours for all steel grades. It is clear from Fig. 11 that the mass gain of steel (1A) is higher than the mass gain for steels (13), (12) and (2A). The difference is the presence of molybdenum in steels (13), (12) and (2A) and absence of molybdenum in steel (1A). This means that the presence of molybdenum (in

chromium content about 25%) improves oxidation behaviour of ferritic stainless steels. The mass gain of steel (2A) is greater than mass gain of steel (12). This confirms the positive effect of vanadium on oxidation behaviour of ferritic stainless steels. Also, it was noticed that steel (13) is higher oxidation resistance than steel (12) as illustrated in Fig. 11. This confirms the positive significant influence of titanium. SEM examination illustrated that the oxidation layer of steel (A2) is not more than 2 μm as illustrated in Fig. 12.

Fig. 13 illustrates the mass gain against time of ferritic stainless steel containing chromium content in range 22.11-23.49%. It is clear that the oxidation rates are large at the beginning up to about 50 hours, and then oxidation rates reach steady state at about 50 hours. Obviously, it is clear that steel (2) has highest mass gain than others steels. This can be attributed to the low vanadium content. Steel (3) has the lowest mass gain as a result of positive significant effect of vanadium (0.051%). Oxidation behaviour of steel (5) was affected by two opposite factors. The positive one is the presence of high vanadium and titanium content and the negative one is the high content of silicon. SEM examination illustrated that the oxidation layer of steel (3) is not more than 10 μm as illustrated in Fig. 14.
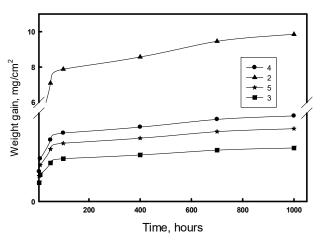

Fig. 13 The variation of mass gain (mg/cm^2) with time (hours) of steel grades of fourth group (4, 2, 5, 3) at 800 ^{o}C up to 1000 hour

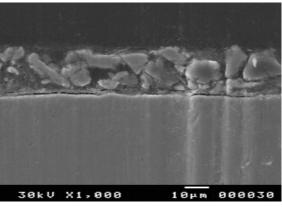

Fig. 14 SEM micrograph of steel (3)

IV. CONCLUSIONS

High temperature oxidation behavior of new developed chromium-steel interconnects for SOFCs has been investigated at 800 °C up to 1000 hours. From the obtained results, it can be concluded that:

- Microstructure showed that all investigated stainless steel grades have ferritic structure. Also, Schaeffler diagram confirmed these results.
- The oxidation rates are fast up to 50 hours and then decrease to reach to steady state at about 100 hours
- In ferritic stainless steels containing 28.8-33.01% Cr, aluminum and silicon have negative effect on oxidation resistance, while addition of titanium improves oxidation behavior.
- In ferritic stainless steels containing 25.5-27.3% Cr, aluminum has negative effect on the oxidation resistance, while addition of vanadium improves oxidation behavior. Molybdenum and niobium have insignificant effect on oxidation behavior.
- In ferritic stainless steels (25.0-25.1% Cr), vanadium, titanium and molybdenum have significant positive effect on oxidation resistance.
- In ferritic stainless steels containing 22.11-23.49% Cr, vanadium has significant positive effect on oxidation resistance.
- The formed oxidation layer could be investigated to 2 µm by adjusting the chemical composition.

REFERENCES

[1] M.C. Williams, J.P. Strakey, W.A. Surdoval, J. Power Sources 143 (1-2) (2005) 191.
[2] V. Karakoussis, N.P. Brandon, M. Leach, R. Van der Rost, J. Power Sources 101 (1) (2001) 10.
[3] L. Antoni, Mater. Sci. Forum 461–464 (2004) 1073–1090.
[4] I. Kosacki, C.M. Rouleau, P.F. Becher, J. Bentley, D.H. Lowndes, Solid State Ionics 176 (2005) 1319–1326.
[5] F. Mauvy, J.-M. Bassat, E. Boehm, J.-P. Manaud, P. Dordor, J.-C. Grenier, Solid State Ionics 158 (2003) 17–28.
[6] J.W. Fergus, Mater. Sci. Eng. A397 (2005) 271–283.
[7] K. Huang, P.Y. Hou, J.B. Goodenough, Solid State Ionics 129 (2000), 237–250.
[8] N. Oishi, Y. Yamasaki, Electrochemical Society Proceedings, vol. 19, 1999, 759–766.
[9] P. Berthod, Oxid. Met. 64 (2005) 235–252.
[10] H. Asteman, J.-E. Svensson, L.-G. Johansson, M. Norell, Oxid. Met. 52 (1999) 95–111.
[11] B.B. Ebbinghuaus, Combust. Flame 93 (1993) 119–137.
[12] T. Brylewski, M. Nanko, T. Maruyama, K. Przybylski, Solid State Ionics 143 (2001) 131–150.
[13] W.J. Quadakkers, J. Piron-Abellan, V. Shemet, L. Singheiser, Mater. High Temp. 20 (2) (2003) 115–127.
[14] M. Han, S. Peng, Z. Wang, Z. Yang, X. Chen, J. Power Sources 164 (2007) 278–283.
[15] G.R. Holcomb, D.E. Alman, Scripta Mater. 54 (2006) 1821–1825.
[16] Z. Yang, M.S. Walker, P. Singh, J.W. Stevenson, T. Norby, J. Electrochem. Soc. 151 (2004) B669–B678.
[17] J.E. Hammer, S.J. Laney, R.W. Jackson, K. Coyne, F.S. Pettit, G.H. Meier, Oxid. Met. 67 (2007) 1–38.
[18] Saeed Ghali, Fathy Baiomy, Mamdouh Eissa, "Investigation the Effect of Nitrogen on Oxidation Behavior of Stainless Steel", 7th European Stainless Steel Conference Science and Market, Como (Italy), 21-23 Sept. 2011.
[19] S. Ghali, M. Eissa, H. El-Faramawy, "Simulation of austenitic stainless steel oxidation containing nitrogen at temperature range 500 °C – 800 °C", International Journal of Statistics and Mathematics, Vol. 1(3), pp. 024-032, August, 2014. © www.premierpublishers.org, ISSN: 2374-0499.
[20] C. Key, J. Eziashi, J. Froitzheim, R. Amendola, R. Smith, and P. Gannon; "Methods to Quantify Reactive Chromium Vaporization from Solid Oxide Fuel Cell Interconnects", Journal of The Electrochemical Society, 161 (9) C373-C381 (2014).
[21] M.O. Speidel and P.J. Uggowitzer: R.A. Lula (ed.), Proc. Materials Week 92, Chicago, ASM Int., p. 135, (1993).
[22] A Ahmed, MK El-Fawakhry, M Eissa, T Mattar, "Thermal compatibility of chromium steel as metallic interconnects for solid oxide fuel cells", Journal of Basic Applied Research International 14 (2), 90-100.
[23] Ravi Shankara, N.S. Karthiselvab, U. Kamachi Mudali, "Thermal oxidation of titanium to improve corrosion resistance in boiling nitric acid Surface and Coatings Technology, Volume 235, 25 November 2013, Pages 45–53.